Ultramicroscopy 000 (2017) 1–5

Contents lists available at ScienceDirect

Ultramicroscopy

journal homepage: www.elsevier.com/locate/ultramic

Comment on, "On the influence of the electron dose-rate on the HRTEM image contrast", by Juri Barthel, Markus Lentzen, Andreas Thust, ULTRAM12246 (2016), http://dx.doi.org/10.1016/j.ultramic.2016.11.016

C. Kisielowski[a,*], H.A. Calderon[b], F.R. Chen[c], S. Helveg[d], J.R. Jinschek[e], P. Specht[f], D. Van Dyck[g]

[a] Lawrence Berkeley National Laboratory, The Molecular Foundry, One Cyclotron Road, Berkeley, CA 94720, USA
[b] Departamento de Física, Instituto Politecnico Nacional ESFM, UPALM-Zacatenco Ed. 9, México CDMX, Mexico
[c] Department of Engineering and System Science, National Tsing-Hua University, 101 Kuang-Fu Road, Hsin Chu 300, Taiwan
[d] Haldor Topsoe A/S, Haldor Topsøes Allé 1, Kgs. Lyngby, DK-2800 Denmark
[e] Department of Materials Science and Engineering, Center for Electron Microscopy and Analysis (CEMAS), The Ohio State University, 1305 Kinnear Rd, Columbus, OH 43212, USA
[f] Department of Materials Science & Engineering, University of California-Berkeley, Berkeley, CA 94720, USA
[g] EMAT, Department of Physics, University of Antwerp, Antwerpen 2020, Belgium

ARTICLE INFO

Article history:
Received 30 January 2017
Accepted 4 April 2017
Available online xxx

In a recent paper Barthel et al. [1] examine the role of the electron dose-rate on the image contrast in high-resolution transmission electron microscopy (HRTEM). It was concluded that the image contrast is independent of the electron dose-rate and that strong electron beam-induced atom displacements from their equilibrium positions are absent that would significantly exceed isotropic Debye–Waller factors $B = 8\pi/3 <u^2>$ at room temperature [1]. These findings stand in marked opposition to our recent reports that the electron dose-rate indeed has a marked influence on the HRTEM image contrast [2–5]. We welcome the opportunity to address the underlying facts and assumptions and find it appropriate to address this apparent discrepancy by demonstrating that the findings in [1] are in fact contained in the results of [2–5], which apply to HRTEM images and to imaging in a Scanning Transmission Electron Microscopy (STEM).

Certainly, we agree that understanding the origin and magnitude of atom displacements is of essence because of its far reaching consequences that touch on the wide spread utilization of Debye–Waller factors to quantitatively describe the contrast in atomic resolution images that are commonly acquired by exposing thin samples to electron doses that can greatly exceed 10,000 e/Å^2. Debye–Waller factors were initially introduced to describe an intensity reduction of Bragg-peaks in diffraction patterns that were recorded with x-rays [6,7]. In electron microscopy experiments, diffraction patterns are typically acquired in low-dose conditions when the samples are illuminated over large areas at small magnification, whereby the electron beam current densities (or dose-rates) are necessarily low. Consequently, it can often be assumed that the thermal occupation of vibrational and electronic states remains unchanged during the image acquisition time. In this case the Born–Oppenheimer approximation [8] is applicable and the impact of temperature on atom displacements is dominant and commonly modeled as a statistical displacement average that forces an exponential decay of scattering vectors ~ exp(-kB).

However, it is unexplored in which imaging conditions and on what time scales the Born–Oppenheimer approximation remains applicable. The concept was recently questioned for investigations that enable sub-Ångstrom resolution with single atom sensitivity in real space images [2–5]. One expects limitations because a detection of single atoms demands a dramatic increase of beam current densities to produce enough elastic Coulomb scattering events of the probing electrons with the nuclei of the investigated material to make atoms visible. Certainly, electron beam current densities can be chosen as low as one e/Å^{2}s for the detection of diffraction patterns in selected area diffraction mode that can be used to

* Corresponding author:.
E-mail address: CFKisielowski@lbl.gov (C. Kisielowski).

http://dx.doi.org/10.1016/j.ultramic.2017.04.002

measure Debye–Waller factors [e.g. 9]. However, they can also exceed 5×10^7 e/Å^{2}s for the acquisition of atomic resolution high angle annular dark field images [2]. Thus, electron microscopy studies employ dose rates that are altered by 7–8 orders of magnitude.

The authors of Ref. [1] probe for contrast alterations in HRTEM images by varying dose-rates over the limited range of $\sim 10^3$–10^5 e/Å^{2}s. These are typical for investigations of bulk materials that were thinned to be electron transparent but remain thick enough so that surface contributions hardly affect the data interpretation. However, an examination of nanostructured materials with greatly increased contributions from surfaces and interfaces forced us to advance the standard detection schemes. Factually, most of our initial results were extracted from single images recorded with the negative spherical-aberration imaging (NCSI) technique and using the TEAM 0.5 microscope, which exhibits a uniquely large information transfer to below 0.5 Å [10]. A Nelsonian illumination system is used to improve on resolution and to match the illuminated sample area to the size of the CCD camera. We expanded the common acquisition practice of single images at a later point of time to include dose-rates as low as 1 e/Å^{2}s, an illuminated sample area that can be more than 100 times smaller than reported in Ref. [1] but remains free of fringes from the presence of apertures, the ability to dramatically alter beam currents by 4–5 orders of magnitude in a fraction of a second without an introduction of uncontrolled lens aberrations, and the ability to correct for residual lens aberrations < 0.5 Å after the acquisition of low-dose-rate image series [2–5,11]. In fact, our reconstructed electron exit wave functions or in-line holograms exhibit an unmatched sub-Ångstrom resolution and superior signal-to-noise ratios (SNRs) even if low-dose-rates <10 e/Å^{2}s are employed that are much too small to capture interpretable information in single high resolution images because of their poor SNRs. With these expanded acquisition schemes, even the genuine structure of nanomaterials including their surfaces and interfaces can be captured in amplitude and phase images unaltered by the delivery of the probing electrons. In contrast, high dose-rates in the regime 10^3–10^5 eÅ^{-2}s^{-1} are often too narrow to reveal the beam-induced sample alterations, in particular if samples are thick [10] and time-dependences are averaged.

Since the two viewpoints differ in the way the HRTEM images are analyzed, we examine first the applicability of the proposed global, spatially averaged contrast measurements of Reference [1]. Linking both approaches, the supplementary Fig. S1 makes use of our published NCSI images from catalytic Rhodium particles (Fig. S1a) that made us reconsider the origin of contrast loss [12]. The reported local intensity variations can be analyzed by extracting e.g. line profiles from image series. Characteristic features of such data sets include local intensity changes up to 50% (Fig. S1b) and random displacements of intensity maxima by 2–50 pm in numerous image locations (Fig. S1c) if a typical electron dose-rate of 7.6×10^3 e/Å^{2}s is applied at 80 kV [12]. Their unexpected large magnitude in thin samples makes such distortions readily observable by visually inspecting image time series and the contrast fluctuations and displacements were explained by reversible object excitations [3]. They were quantitatively modeled using frozen phonon multislice calculations that simulate random, long-lasting atom displacements up to 50 pm in three dimensions. Movies of the observed electron beam-induced structure alterations are published on-line [10], including a movie of image simulations that show how random and temporarily stabilized atom configurations affect the image contrast if the sample thicknesses increases. A logarithmic gain of image contrast by a factor of ~2 was observed if dose-rates are dropped from 6000 to 40 e/Å^{2}s [3]. Low-dose rates are targeted because our investigations aim at including the low-dose imaging conditions that are established for damage-free imaging of nanostructured and biological materials (<20 e/Å^2) that are susceptible to alterations by the electron beam [13]. In stark contrast, global image contrast measurements as suggested in Reference [1] do not capture any of the beam-induced structural dynamics. Instead, the example at hand yields a remarkably constant contrast value of 0.162 ± 0.007 for any of the 36 experimental images if analyzed as suggested (Fig. S1d). However, if we calculate an average image contrast from all recorded 36 frames, the average contrast is ~ 30% smaller than the contrast in any single image, which reveals the presence of beam-induced object alterations on a time scale of seconds. Since current image alignments schemes in HRTEM to a precision of the electron wavelength (1.9 pm at 300 kV) assume that only the entire image frames shift with respect to each other, a local displacement of intensity maxima by much more than 2 pm causes contrast blur and reduction. In Reference [3] such random intensity displacements were reduced from 65 pm to 35 pm upon lowering the beam current density from 6000 to 40 e/Å^{2}s. Their reduction necessarily causes the reported contrast gain in exit wave functions that were reconstructed from aligned low-dose-rate images.

Thus, the authors of Reference [1] apply a protocol that is insensitive to the time dependent structure reconfigurations that occur with frequencies of 1–10 Hz in high dose-rate imaging conditions. Obviously, such frequencies are much lower than the typical vibrational frequencies of atoms and their origin is of interest. In Reference [1] the implicit assumption seems to be that beam-current densities of 10^3 and 10^5 e/Å^{2}s hardly affect the population of vibrational states with energies around $kT = 25$ meV at room temperature and that contrast maxima of atom column positions remain constant to within ~ 2 pm. These assumptions would hold in low-dose-rate conditions where the Born–Oppenheimer approximation remains valid, but they break down if structural reconfigurations are induced by the probing electron beam, which is what we revealed by analyzing time series of single high dose-rate images [3,12]. In principle, the use of spatial averaged versus local intensity measurements resolves the seemingly contradicting views between [1] and [2–5] that beam-induced atom displacements are detectable in the image contrast. However, it is also needed to reconsider the measurements of Ge, Au and MgO in more detail because the authors of [1] argue that typical Debye–Waller factors are not overwritten in high resolution images of these materials by beam-induced object excitations if dose-rates beyond ~ 1000 e/Å^{2}s are employed and their impact on the interpretation of single images would be undetectable.

For this purpose, the Fig. 1 details results of the published multislice simulations of Rh [110] for different sample thicknesses [10, movie] that allow observing the beam-induced atom displacements by a visual image inspection because of their large magnitude. A single image of one simulated atom configuration is reproduced in Fig. 1a. It was generated using three-dimensional frozen phonon simulations with up to 50 pm random atom displacements in three dimensions. Further, it is assumed that the visible distortions are temporarily stabilized for reasons that will be discussed later, so that a distorted structure can be captured with an exposure time around a second. The Fig. 1d is produced by applying the proposed contrast measurements [1] to our simulated images and by extracting a local contrast width σ by fitting Gaussian functions to the local intensities of atoms and atom columns. It is seen that the global contrast increases with sample thickness to largest values of 0.4–0.5 in optimized imaging conditions (blue triangles in Fig. 1d). A multislice calculation of extinction distances ζ confirms that the largest contrast values occur around $\zeta/4$. In Rh [110], the related sample thickness is only ~ 1 nm (4 atomic layers) because the simulations and the matching experiments were executed with an electron acceleration voltage of only 80 kV. Simultaneously, one finds that the contrast width (black squares in Fig. 1d) is reduced by ~ 10 pm with increasing sample thickness, an effect that is caused by a combination of averaging the frozen phonon contribu-

Please cite this article as: C. Kisielowski et al., Comment on, "On the influence of the electron dose-rate on the HRTEM image contrast", by Juri Barthel, Markus Lentzen, Andreas Thust, ULTRAM12246 (2016), http://dx.doi.org/10.1016/j.ultramic.2016.11.016, Ultramicroscopy (2017), http://dx.doi.org/10.1016/j.ultramic.2017.04.002

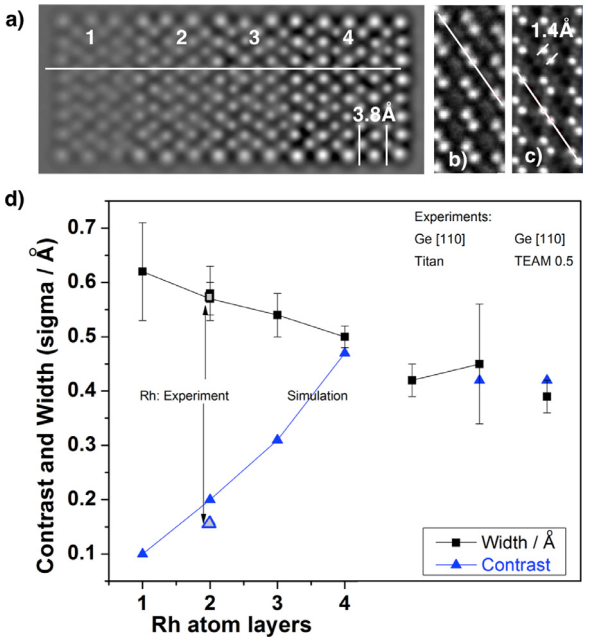

Fig. 1. Global contrast (blue triangles) and contrast width (black squares) measurements of published images from Rh [110] (simulation) [10] and Ge [110] (experiments) from References [1,14]. 1 Å wide line profiles were extracted along the white lines to measure the local contrast width. (a) A simulated NCSI image of one specific atom configuration of the movie published in [10]. A Rh [110] wedge is shown containing 1 - 4 atomic layers. Random atom displacements up to 50 pm in three dimensions are included in each of the layers. The global contrast is extracted from each terrace of the simulation. (b) An experimental NCSI image of Ge[110] from Ref. [1], dose rate: 32×10^3 e/Å^{2}s (c) An experimental NCSI image of Ge[110] from Ref. [14], dose rate: 26×10^3 e/Å^{2}s (d) Global contrast and contrast width measurements for the displayed images. An experimental result for Rh[110] is included in the data showing that a theory allows for large atom displacements fits the experiments well. (For interpretation of the references to colour in this figure legend, the reader is referred to the web version of this article.)

tions in each layer and electron channeling. In any case, the simulated 50 pm large atom displacements are neither visible nor directly accessible in the images of thicker sample areas even though they are included in every simulated atomic layer. Instead, time series of images capture the atom motion best in thin samples as demonstrated in the movie and in single images one expects to detect a contrast width that increases with decreasing sample thickness but can hardly be affected by improving on sub-Ångstrom resolution. Thus, it is unfortunate but understandable that local, temporal intensity alterations cannot be tracked by the proposed global contrast measurements. In Fig. 1d we compare these expectations with contrast and contrast width measurements of Ge [110] from Reference [1] (Fig. 1b) and from our own measurements [5, 14] (Fig. 1c). It is seen that the similarity of both results is striking. In addition it is remarkable how detailed the measurements reproduce the features that are modeled for Rh [110] if scaled with the extinction distance. For 300 kV one calculates that the Ge [110] sample thickness at $\zeta/4$ is $\sim$ 5 nm (columns contain $\sim$ 12 atoms), which provides a global contrast around 0.4 in direct images of the atomic structure. Experimentally, the reference [14] reports a thickness dependence of the contrast width from single images of Ge [110] that it is 14 pm and 8 pm in 2 nm and $\sim$7 nm thick samples, respectively. The result is in full agreement with our expectations from the Rh [110] image simulations that also predict a $\sim$ 10 pm width reduction with increasing sample thickness. In addition, the contrast width $\sigma = 0.4$ Å (FWHM $= 2.4 \times 40$ pm $= 0.95$ Å) is similar in both experiments. The latter is unexpected because the TEAM 0.5 microscope exhibits an improved resolution and stability if compared to a TITAN instrument. An almost identical contrast widths is compatible with the view that it is more affected by beam-induced atom displacements than it is affected by resolution as one expects from the Rh [110] simulations, too. Naturally, it will always remain challenging to measure a narrowing of contrast of atom columns if the microscope resolution is a limiting factor. The contrast of Ge columns exhibits a FWHM of 0.95 Å The resolution of TITAN instruments is close to 0.8 Å but for TEAM 0.5 it is better than 0.5 Å In summary, we cannot find any contradiction between the measurements reported in Ref [1] and our interpretation of image contrast.

Next, we address the case of a gold crystal together with the claim that such effects would not be visible in STEM measurements. For this purpose we provide a movie of successive STEM images in the supplementary information that were recorded with quite typical beam currents around 50 pA and with a dwell times around 10 µs [15]. As in the cases of Rh and Ge, it is seen that single images tend to show a static column arrangement. Image sequences, however, reveal the same effects of beam-induced atom dynamics: The atom columns at the thin edge of the wedge shaped sample are randomly displaced from image to image by distances as large as 30–50 pm so that the crystal structure appears to be dissolved in the thin areas close to the sample surface. Nevertheless, the atomic structure in thicker crystal areas is seemingly unaffected if judged by visual image inspections. There, global contrast measurements are also constant in a given field of view. Nevertheless, the pronounced beam-induced grain boundary rotation at room temperature proves at that even in the thick sample areas the deposited beam energy exceeds the thermal contributions and necessarily induces structural reconfigurations and local atom diffusion on a time scale of Hz that do not occur at room temperature. Thus, a careful inspection of image series reveal that STEM images exhibit the presence of beam induced atom dynamics, too, in contrast to the opposite claims of Reference [1]. Again, we cannot find contradiction concerning our interpretation of image contrast.

Beyond methodical considerations, the magnitude of Debye–Waller factors is especially relevant for the interpretation of image contrast in electron tomography, which was performed with MgO [5,16]. If Debye–Waller factors are chosen too small in image simulations it becomes possible to describe an experimental image contrast with fewer atoms in columns. Resultantly, the sample thickness is underestimated if the experimental image contrast is quantitatively matched to simulations. Such a discrepancy has occurred for thickness measurements from the MgO tomograms of References [5] and [16] where images of similar contrasts around 0.4 are present at the very edge of the considered samples in both cases. For MgO a quarter of an extinction distance is calculated to be 11.5 nm at 300 kV. Indeed, a sample thickness of $\sim$ 10 nm is reconstructed using the self consistent method of Ref. [5] but it is surprisingly only 2 - 2.5 nm small in Ref. [16], where the thickness determination includes a comparison with theory using Debye–Waller factors for room temperature. We also point out the inconsistency that in our experience [10] a 2–2.5 nm thin area is very susceptible to a rapid loss of structural integrity if exposed to beam current densities as large as $\sim$ 70,000 e/Å^{2}s in Reference [16].

Surely, the most relevant discrepancy relates to our assumed stabilization of excited atom configurations on a time scale of Hz while atom vibrations can obviously exceed frequencies of GHz. We underscore our view that collective atom excitation can provide a temporary stabilization of excited object configurations by summarizing the published results of Molecular Dynamics simulations of collective atom excitations in graphene that were used to explain the measured contrast by matching experiments with simulations in Reference [3]. There, graphene was chosen because its two-dimensionality offers low spatial restrictions to large atom

Please cite this article as: C. Kisielowski et al., Comment on, "On the influence of the electron dose-rate on the HRTEM image contrast", by Juri Barthel, Markus Lentzen, Andreas Thust, ULTRAM12246 (2016), http://dx.doi.org/10.1016/j.ultramic.2016.11.016, Ultramicroscopy (2017), http://dx.doi.org/10.1016/j.ultramic.2017.04.002

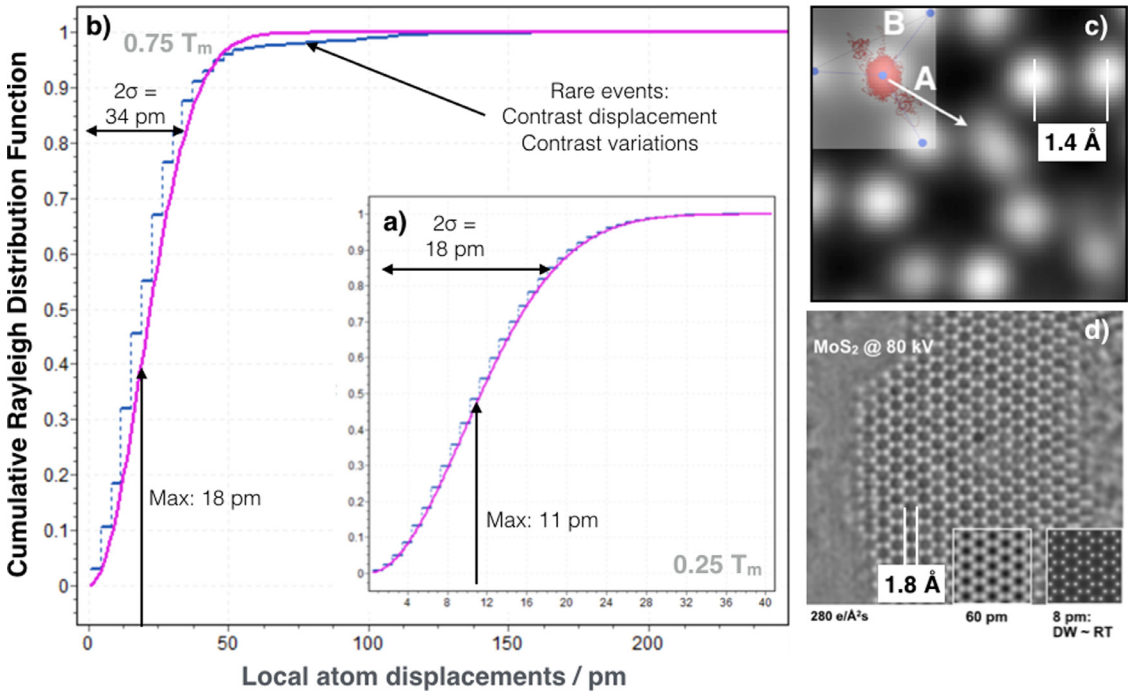

Fig. 2. Electron beam-induced atom motion in 2D materials. (a) Collective atom displacements in graphene predicted by molecular dynamics simulations at $T_m/4$, T_m= melting point temperature [3]. In plane and out of plane atom displacements are simulated. A cumulated Rayleigh distribution function is fitted to the simulated data to highlight the good match. (b) Same as in (a) but at an increased temperature of $3T_m/4$. The occurrence of large displacements is pointed out (rare events) that cause deviations from the fitted distribution function. (c) An image simulation using the simulated $3T_m/4$ data to show that rare events contribute to the experimentally detected contrast blur [3]. (d) Experimental contrast blur in a reconstructed electron exit wave function of MoS_2 (phase image). Image simulations are shown as insets to be compared to the experimental contrast. Typical atom vibrations around 8 pm match Debye–Waller factors but greatly fail to describe the image contrast. Local displacements of 60 pm allow describing the image contrast quantitatively but largely exceed typical Debye–Waller factors at room temperature.

displacement due to the reduced atom coordination. These simulations can also be directly compared to recent measurements of Debye–Waller factors between 300 K and 1300 K from diffraction patterns [9]. In-plane atom displacements $u_{x,y}$ between 4 pm and 6 pm are reported and out-of-plane values u_z reach from 10 to 24 pm. From Fig. 2a it is clear that these measured Debye–Waller factors are entirely compatible with our calculated atom displacements $u^2 = u_{x,y}{}^2 + u_z{}^2$ [3] that closely follow the fitted cumulative Rayleigh distribution function at low temperature. However, an increasing temperature gives rise to unusual large atom displacements (rare events) that temporarily stabilize unexpected atom configurations as pointed out in Fig. 2b. In the case of graphene they cause an additional image blur that is simulated in Fig. 2c and can be picked up experimentally [3]. Beyond graphene, contrast broadening in 2D materials is common and is exceptionally well visible in images of MoS_2 because of the large Mo - S dumbbell separation of 1.8 Å in a (0001) projection of the structure as shown in Fig. 2d. The experimental images can certainly not be matched by simulations using typical Debye–Waller factors that describe 5–10 pm of atom displacements (Fig. 2d, inset), and contributions from a limited instrumental resolution are negligible in this case. Instead, beam-induced atom displacements must be as large as 60 pm to match the experimental image contrast as shown in the inset of Fig. 2d, too.

From a physical point of view, it is also disadvantageous to ignore beam-induced object excitations since they allow studying dynamic responses of matter at the atomic scale. Relevant time constants can greatly vary because the stabilization of a specific atom configuration is determined by existing energy barriers that must be overcome by the beam-induced atom displacement or by an occurrence of bond ionization events. Selected examples of such processes are the excitation of single Rh atoms from the bulk lattice sites into the (110) surface corrugation of nanocrystals across barriers of 0.1 and 1.0 eV [3]; the reported excitation of two different structural configurations of a boron vacancy in a double layer of BN across an energy gap of ~ 500 meV [17]; the beam induced diffusion of atoms in cadmium sulfide/copper sulfide with activation energies of 230 meV or 960 meV [18], or simply the direct observation of beam induced grain rotations [2], the detection of Oswald ripening in thin films [19] and its suppression by choosing a suitably low-dose rate [20].

In summary, we respond to the discussion in Reference [1] that it focuses on an inappropriately narrow range of dose-rates and applies a global contrast measurement scheme that is quite insensitive to beam-induced object alterations. The relevant low-dose regime could not be accessed in the comment because of unavoidable noise limitations in single images. Further, the difference between local contrast fluctuations and a global image contrast must be taken into account since it is neither obvious nor established how local electron beam-induced object excitations affect the global image contrast. Upon clarifying this difference, it is shown that a recording of image time series efficiently captures the large atom displacements which are attributed to reversible system excitations in high dose-rate conditions. They induce conformational object changes that challenge the Born–Oppenheimer approximation. In this process, the traditional room temperature Debye–Waller factors for periodic structures are commonly overwritten even if moderate dose-rates are chosen around ~ 100 e/Å^{2}s to acquire high resolution images. Our view is also consistent with reports on amorphous materials where the large electron beam-induced atom displacements can be detected in image time series, too, causing displacement decoherence [21].

Please cite this article as: C. Kisielowski et al., Comment on, “On the influence of the electron dose-rate on the HRTEM image contrast”, by Juri Barthel, Markus Lentzen, Andreas Thust, ULTRAM12246 (2016), http://dx.doi.org/10.1016/j.ultramic.2016.11.016, Ultramicroscopy (2017), http://dx.doi.org/10.1016/j.ultramic.2017.04.002

Acknowledgment

Electron microscopy is supported by the Molecular Foundry, which is supported by the Office of Science, the Office of Basic Energy Sciences, the U.S. Department of Energy under Contract No. DE-AC02-05CH11231.

Supplementary materials

Supplementary material associated with this article can be found, in the online version, at doi:10.1016/j.ultramic.2017.04.002.

References

[1] J. Barthel, M. Lentzen, A. Thust, On the influence of the electron dose-rate on the HRTEM image contrast, Ultramicroscopy (2016), http://dx.doi.org/10.1016/j.ultramic.2016.11.016 ULTRAM12246.
[2] C. Kisielowski, H. Frei, P. Specht, I.D. Sharp, J.A. Haber, S. Helveg, Detecting structural variances of Co3O4 catalysts by controlling beam-induced sample alterations in the vacuum of a transmission electron microscope, Adv. Struct. Chem. Imaging 2 (2016) 13.
[3] C. Kisielowski, L-W. Wang, P. Specht, H. Calderon, B. Barton, B. Jiang, J.H. Kang, R. Cieslinski, Real-time sub-Ångstrom imaging of irreversible conformations in rhodium catalysts and graphene, Phys. Rev. B 88 (2013) 024305.
[4] D. Van Dyck, I. Lobato, F.-R. Chen, C. Kisielowski, Do you believe that atoms stay in place when you observe them in HREM? Micron 68 (2014) 158–163.
[5] F.-R. Chen, D. Van Dyck, C. Kisielowski, In-line three-dimensional holography of nanocrystalline objects at atomic resolution, Nat. Commun. 7 (2016) 10603.
[6] P. Debye, Interferenz von Roentgenstrahlen und Waermebewegung, Annalen der Physik 348 (1913) 49–92.
[7] I. Waller, Zur Frage der Einwirkung der Waermebewegung auf die Interferenz von Roentgenstrahlen, Zeitschrift fuer Physik 17 (1923) 398–408.
[8] M. Born, R. Oppenheimer, Zur Quantentheorie der Molekeln, Annalen der Physik 84 (1927) 457–484.
[9] C.S. Allen, E. Liberti, J.S. Kim, Q. Xu, Ye Fan, K. He, A.W. Robertson, H.W. Zandbergen, J.H. Warner, A.I. Kirkland, Temperature dependence of atomic vibrations in mono-layer graphene, J. Appl. Phys. 118 (2015) 074302.
[10] C. Kisielowski, P. Specht, S.M. Gygax, B. Barton, H.A. Calderon, J.H. Kang, R. Cieslinski, Instrumental requirements for the detection of electron beam-induced object excitations at the single atom level in high-resolution transmission electron microscopy, Micron 68 (2015) 186–193.
[11] B. Barton, B. Jiang, C.-Yu Song, P. Specht, H. Calderon, C. Kisielowski, Atomic-resolution phase-contrast imaging and in-line electron holography using variable voltage and dose rate, Microsc. Microanal. 18 (2012) 982–994.
[12] Petra Specht, RobertJ. Gulotty Jr., David Barton, Robert Cieslinski, Steve Rozeveld, JooH. Kang, Oscar.D. Dubon, Christian Kisielowski, Quantitative contrast evaluation of an industry-style rhodium nanocatalyst with single atom sensitivity, ChemCatChem 3 (2011) 1034–1037.
[13] E. Callaway, The revolution will not be crystallized, Nature 525 (2015) 172–174.
[14] D. Alloyeau, B. Freitag, S. Dag, Lin.W. Wang, C. Kisielowski, Atomic-resolution three-dimensional imaging of germanium self-interstitials near a surface: aberration-corrected transmission electron microscopy, Phys. Rev. B 80 (2009) 014114.
[15] R. Erni, M.D. Rossell, C. Kisielowski, U. Dahmen, Atomic-resolution imaging with a sub-50-pm electron probe, Phys. Rev. Lett. 102 (2009) 096101.
[16] C.L. Jia, S.B. Mi, J. Barthel, D.W. Wang, E. Dunin-Borkowski, K.W. Urban, A. Thust, Determination of the 3D shape of a nanoscale crystal with atomic resolution from a single image, Nat. Mat. (2015), doi:10.1038/NMAT4426.
[17] N. Alem, O.V. Yazyev, C. Kisielowski, P. Denes, U. Dahmen, P. Hartel, M. Haider, M. Bischoff, B. Jiang, S.G. Louie, A. Zettl, Probing the out-of-plane distortion of single point defects in atomically thin hexagonal boron nitride at the picometer scale, Phys. Ref. Lett. 106 (2011) 126102.
[18] H. Zheng, B. Sadtler, C. Habenicht, B. Freitag, A. Paul Alivisatos, C. Kisielowski, Controlling electron beam-induced structure modifications and cation exchange in cadmium sulfide-copper sulfide heterostructured nanorods, Ultramicroscopy 134 (2013) 207–213.
[19] J. Yang, J.K. Cooper, F.M. Toma, K.A. Walczak, M. Favaro, J.W. Beeman, L.H. Hess, C. Wang, C. Zhu, S. Gul, J. Yano, C. Kisielowski, A. Schwartzberg, I.D. Sharp, A multifunctional biphasic water splitting catalyst tailored for integration with high-performance semiconductor photoanodes, Nat. Mater. (2016), doi:10.1038/NMAT4794.
[20] S.B. Simonsen, I. Chorkendorff, S. Dahl, M. Skoglundh, J. Sehested, S Helveg, Direct observations of oxygen-induced platinum nanoparticle ripening studied by in situ tem, J. Am. Chem. Soc. 132 (2010) 7968–7975.
[21] A. Rezikyan, Z.J. Jibben, B.A. Rock, G. Zhao, F.A.M. Koeck,1, R.F. Nemanich, M.M.J. Treacy, Speckle suppression by decoherence in fluctuation electron microscopy, Microsc. Microanal. 21 (2015) 1455–1474.

Please cite this article as: C. Kisielowski et al., Comment on, “On the influence of the electron dose-rate on the HRTEM image contrast”, by Juri Barthel, Markus Lentzen, Andreas Thust, ULTRAM12246 (2016), http://dx.doi.org/10.1016/j.ultramic.2016.11.016, Ultramicroscopy (2017), http://dx.doi.org/10.1016/j.ultramic.2017.04.002